

## A CLUMPING-INDEPENDENT DIAGNOSTIC OF STELLAR MASS-LOSS RATES: RAPID CLUMP DESTRUCTION IN ADIABATIC COLLIDING WINDS

J. M. PITTARD<sup>1</sup>

Received 2007 February 26; accepted 2007 March 22; published 2007 April 17

### ABSTRACT

Clumping in hot star winds can significantly affect estimates of mass-loss rates, the inferred evolution of the star, and the environmental impact of the wind. A hydrodynamical simulation of a colliding winds binary (CWB) with clumpy winds reveals that the clumps are rapidly destroyed after passing through the confining shocks of the wind-wind collision region (WCR) for reasonable parameters of the clumps if the flow in the WCR is adiabatic. Despite large density and temperature fluctuations in the postshock gas, the overall effect of the interaction is to smooth the existing structure in the winds. Averaged over the entire interaction region, the resulting X-ray emission is very similar to that from the collision of smooth winds. The insensitivity of the X-ray emission to clumping suggests it is an excellent diagnostic of the stellar mass-loss rates ( $\dot{M}$ ) in wide CWBs and may prove to be a useful addition to existing techniques for deriving  $\dot{M}$ , many of which are extremely sensitive to clumping. Clumpy winds also have implications for a variety of phenomena at the WCR: particle acceleration may occur *throughout* the WCR due to supersonic MHD turbulence, reacceleration at multiple shocks, and reconnection; a statistical description of the properties of the WCR may be required for studies of non-equilibrium ionization and the rate of electron heating; and the physical mixing of the two winds will be enhanced, as seems necessary to trigger dust formation.

*Subject headings:* hydrodynamics — stars: individual (WR 140) — stars: mass loss — stars: winds, outflows — stars: Wolf-Rayet — X-rays: stars

### 1. INTRODUCTION

There is now considerable observational evidence for a high degree of structure, or “clumping,” in hot stellar winds (e.g., Moffat et al. 1988; Lepine et al. 2000). Clumping affects diagnostics of mass-loss rates that are sensitive to the square of the density (e.g., free-free radio, infrared continuum,  $H\alpha$ ). If not taken into account, the inferred mass-loss rates may be substantially above their actual values. For Wolf-Rayet (WR) stars, the assumption of a smooth wind typically leads to a factor of 3 overestimate. Recent studies are now indicating that the winds of main-sequence stars may be even more structured, and downward revisions in  $\dot{M}$  by factors of 3–10 or more have been suggested (e.g., Bouret et al. 2005; Fullerton et al. 2006; Puls et al. 2006). Such substantial reductions have a dramatic effect on the evolution and environmental impact of massive stars and may also be needed to explain the near-symmetry of X-ray lines (Owocki & Cohen 2006).

Several methods for determining mass-loss rates that are not sensitive to  $\rho^2$  are unique to binary systems. First, if the period of the binary is short enough, and the mass-loss rates high enough,  $\dot{M}$  can be determined from the observed change in the orbital period. Although this has been applied to the WR binary V444 Cyg (e.g., Antokhin et al. 1995), it has limited applicability. Observed changes in polarization and atmospheric continuum eclipses can also be used to determine mass-loss rates (St.-Louis et al. 1988; Lamontagne et al. 1996).

Measurements of  $\dot{M}$  have also been made by comparing the observed X-ray flux arising from the WCR to predictions from hydrodynamical models of this interaction (Stevens et al. 1996; Pittard & Corcoran 2002; Pittard & Dougherty 2006). In all of these models, homogeneous winds were assumed, but this work shows that structured winds are rapidly smoothed out in the WCR of *wide* binaries: hence, the X-ray emission, despite being

sensitive to  $\rho^2$ , is an excellent diagnostic of the actual mass-loss rates. Further implications of wind structure on the interaction region are discussed in § 4.

### 2. CLUMP-WCR INTERACTION

The survival time of a clump within the WCR depends predominantly on its size and density contrast to the mean flow. The low amplitude of detected variability argues for a large number of clumps, each of which is likely to have a quite small spatial scale (e.g., Eversberg et al. 1998; Marchenko et al. 2006 and references therein). If the interclump medium is devoid of material, the density contrast of the clumps relative to the corresponding smooth flow is inversely related to the volume filling factor,  $f_v$ , which the clumps occupy. The value of  $f_v$  initially decreases with radius (i.e., the wind becomes increasingly clumpy), reaches a minimum at around  $(10\text{--}15)R_{*}$ , and then increases as the wind slowly smooths out (Puls et al. 2006). At very large distances, Runacres & Owocki (2005) find that  $f_v \sim 0.25$ .

Clumps that pass into the WCR lose mass primarily through dynamical instabilities (e.g., Kelvin-Helmholtz). The destruction timescale of nonradiative clumps can be parameterized as  $t_d = \epsilon r_c / v_s$  (Klein et al. 1994), where  $r_c$  is the clump radius and  $v_s$  is the shock velocity (for the stationary shocks in CWBs,  $v_s$  is equal to the normal component of the preshock wind speed);  $\epsilon \approx 3.5$  for a density ratio between the clump and interclump wind of order 10–100. A detailed review of clump destruction processes, including the effects of radiative cooling and magnetic fields, can be found in Pittard (2007).

Consider a clump moving along the line of centers between the stars. As the clump passes through one of the shocks confining the WCR, it is decelerated less than the interclump material and pushes the confining shock into the WCR. A lower limit on the timescale for the clump to half-cross the WCR is  $t_{cd} = \Delta r / v_s$ , where  $\Delta r$  is half the distance between the confining shocks. Clumps will be destroyed before they reach this half-

<sup>1</sup> School of Physics and Astronomy, University of Leeds, Leeds, UK; jmp@ast.leeds.ac.uk.

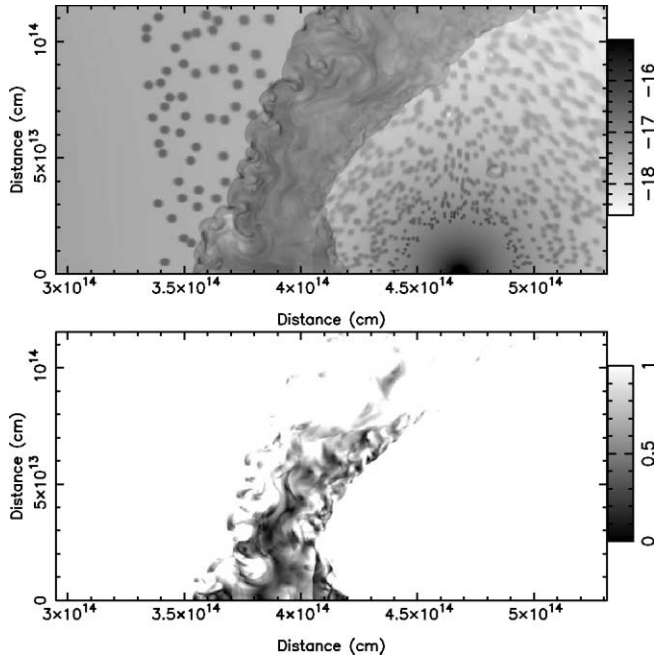


FIG. 1.—*Top*: Logarithmic density plot ( $\log \text{ g cm}^{-3}$ ) from an axisymmetric simulation of colliding clumped winds in WR 140. *Bottom*: Same as the top panel but showing the Mach number of the gas. Supersonic gas is white. Due to the pressure gradients within the WCR, the gas, on average, becomes supersonic as it leaves the system.

way point when  $t_d/t_{cd} = \epsilon r_c/\Delta r < 1$ . Since it is expected that  $r_c \lesssim \Delta r$ , clumps should be rapidly destroyed within the WCR.

### 3. HYDRODYNAMICAL SIMULATIONS

The long-period CWB WR 140 forms the basis of this investigation into the effects of clumpy winds on the interaction region. WR 140 is the archetype of long-period CWBs, exhibiting dramatic variations in its X-ray (Pollock et al. 2005) and radio emission (Dougherty et al. 2005) modulated by its highly eccentric orbit. The emission from radio to TeV energies has recently been modeled by Pittard & Dougherty (2006).

There have been two previous studies of the clumpy colliding winds in WR 140. Walder & Folini (2002) examined a simulation with the stars near periastron. WR material both in and between the clumps rapidly cools and is compressed to high densities. Aleksandrova & Bychkov (2000) considered the transition between periastron and apastron in an attempt to explain the variation of the X-ray flux with the stellar separation.

In this work, the effect of clumpy winds on the WCR is examined when the stars are at apastron (i.e., the stellar separation  $D = 4.7 \times 10^{14}$  cm). The mass-loss rates and terminal wind speeds adopted are  $\dot{M}_{\text{WR}} = 4.3 \times 10^{-5} M_{\odot} \text{ yr}^{-1}$ ,  $\dot{M}_{\text{O}} = 8.0 \times 10^{-7} M_{\odot} \text{ yr}^{-1}$ ,  $v_{\infty, \text{WR}} = 2860 \text{ km s}^{-1}$ ,  $v_{\infty, \text{O}} = 3100 \text{ km s}^{-1}$ . In order to focus attention on the apex of the WCR, which is bent sharply around the O star, the WR star is positioned off the two-dimensional hydrodynamic grid, which is axisymmetric and contains  $1650 \times 660$  cells. The clumps are added to the flow in annuli around each star at specific time intervals. For simplicity, the clumps are assigned the wind terminal speed and have radii proportional to their distance from their star. The clump radius,  $r_c$ , is  $0.005r$  in the WR wind and  $0.02r$  in the O wind, so that the clumps have  $\geq 10$  cells across their radius when interacting with the WCR. The clumps are given a density contrast of 10 with respect to the interclump medium, and the clump and interclump medium are assumed to contain equal mass (hence  $f_v = 1/11$ ). The interclump

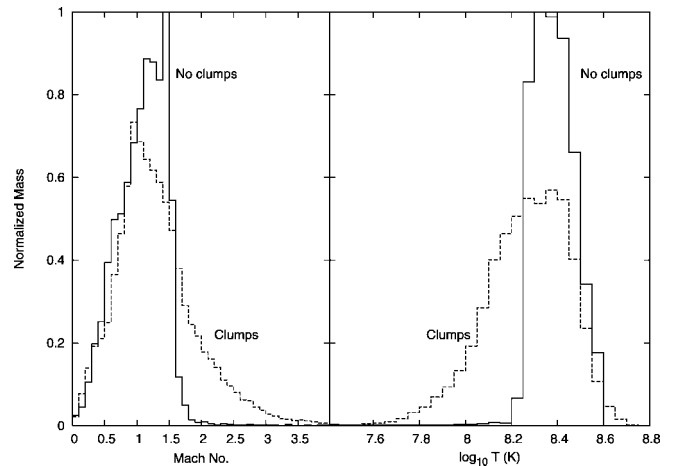


FIG. 2.—*Left*: Comparison of mass as a function of Mach number from simulations with homogeneous (*solid line*) and clumpy (*dashed line*) winds. *Right*: Same as the left panel but as a function of temperature.

medium is perfectly smooth. A simulation with smooth winds reveals that the width of the WCR on the line between the centers of the stars is  $0.0695D$ . Hence,  $t_d/t_{cd} \approx 0.5$  (0.25) for the clumps in the WR (O) wind, and the WCR should quickly smooth out these inhomogeneities.

The hydrodynamical code is second-order accurate in space and time (Falle & Komissarov 1996). Optically thin radiative cooling is included, although radiation losses are negligible. Heat conduction is not explicitly included and is likely to be strongly inhibited by the magnetic field revealed by the synchrotron emission. The clumps are initially spherical, but the velocity dispersion in the radial and transverse directions may differ;  $v_{\theta}/v_r \approx 4$  for the clumps in the O wind, so that they naturally “pancake” as they are advected by the wind. Recent models of X-ray wind absorption support radially compressed rather than spherical clumps (Oskinova et al. 2006). The density contrast of the clumps is also reduced by numerical diffusion. These two effects reduce the survival time of the clumps but are not thought to be significant.

A density plot of the WCR is shown in Figure 1 (*top*). It is immediately evident that the process of clump destruction induces a multitude of large- and small-scale motions within the WCR. This “turbulence,” some of which is supersonic (Fig. 1, *bottom*, and Fig. 2, *left*), puffs up the WCR, so that its volume is 25% larger than the homogeneous case. Temperatures higher than in the smooth-wind case occur when the WCR expands upstream into the relatively low ram pressure of the interclump medium and also behind the bow shocks driven ahead of the clumps. In contrast, the interiors of clumps are initially heated to significantly lower temperatures as shocks driven into them are much slower (shocks driven into clumps in the WR wind near the line of centers have speeds  $\sim 1000 \text{ km s}^{-1}$  and produce temperatures of  $\sim 4 \times 10^7 \text{ K}$ ). Thus, there is a wider distribution of temperatures within the WCR than in the smooth winds case (Fig. 2, *right*).

As cool material within recently shocked clumps moves deeper into the WCR, it is heated by secondary shocks and through mixing with hotter plasma. At any particular instant, the majority of the mass within the WCR is heated to temperatures similar to those that exist in the smooth winds simulation: the mass-weighted mean temperature of gas within the WCR (and on the grid) is  $2.4 \times 10^8$  and  $2.0 \times 10^8 \text{ K}$  for the smooth and structured winds cases, respectively. The average

density in the WCR is similar to the smooth winds case and is not markedly different with 90% of the mass in clumps.

Although the WCR is clearly not smooth, the wind-wind collision decreases the small-scale structure in the winds. Clump disruption is mostly through the development of large-scale perturbations, while the mixing of the clump and interclump material is affected by smaller scale motions. The global nature of the simulation inevitably leads to relatively poor spatial resolution at the scale of individual clumps and is likely to enhance the mixing due to nonnegligible numerical diffusion. In contrast, the lack of a third dimension in these simulations (the imposition of axisymmetry means that the clumps are donut-shaped) should slow the rate of clump destruction as there is 1 less degree of freedom for dynamical instabilities. Resolution tests and comparison with previous work on shock-cloud interactions indicate that these effects do not have a serious impact on the results.

In reality, clumps will possess a variety of density contrasts and sizes—large, dense clumps will survive longer as distinct entities within the WCR than smaller, less dense clumps, although denser clumps may on average be smaller and vice versa (Moffat 1994). If  $t_d/t_{c,d} \gg 1$ , clumps could, in theory, pass completely through the WCR and into the preshock wind of the companion star, but this is unlikely to occur in the wide, adiabatic systems considered here.

### 3.1. Determining Mass-Loss Rates

Since the wind structure is rapidly smoothed, it is not surprising that the X-ray emission is similar to the homogeneous case (Fig. 3). The mean continuum flux at 1 keV is only 17% higher in the clumpy winds simulation, which translates into an 8% overestimate of the mass-loss rates ( $f_x \propto \dot{M}^2$ ). Clearly, there is potential to use the X-ray emission from the WCR as a diagnostic of the stellar mass-loss rates.

However, the structure within the WCR and the resulting X-ray emission depend on the properties of the clumps. Further simulations (J. M. Pittard 2007, in preparation) reveal that the emission measure ( $\int n^2 dV$ ) appears to increase with the clump density contrast: an identical simulation with a density contrast of 100 yields a 56% overestimate of  $\dot{M}$  for each star, but the density contrast is unlikely to be this high in wide CWB systems. Instead, the major sources of uncertainty are likely to be the abundances and the wind momentum ratio,  $\eta$  (as the emission is nearly degenerate between  $\eta$  and the  $\dot{M}$ 's—see Pittard & Dougherty 2006). Nevertheless, X-ray-derived mass-loss rates should be accurate to within a factor of 2. Substantially higher precision may be obtained if  $\eta$  and the wind abundances are strongly constrained.

The level of X-ray absorption by the intervening wind(s) can also, in principle, be used to determine mass-loss rates. For the wide binaries considered here, the clumps are likely to be optically thin, so that the optical depth will be identical to the smooth winds case. However, again there is a degeneracy with  $\eta$  if the line of sight into the system is not well constrained, in which case it may be best to simply match the X-ray flux at energies above those susceptible to absorption (Pittard & Dougherty 2006).

## 4. FURTHER IMPLICATIONS

The interaction of clumpy, as opposed to homogeneous, winds has implications for a variety of phenomena that occur at or within the WCR.

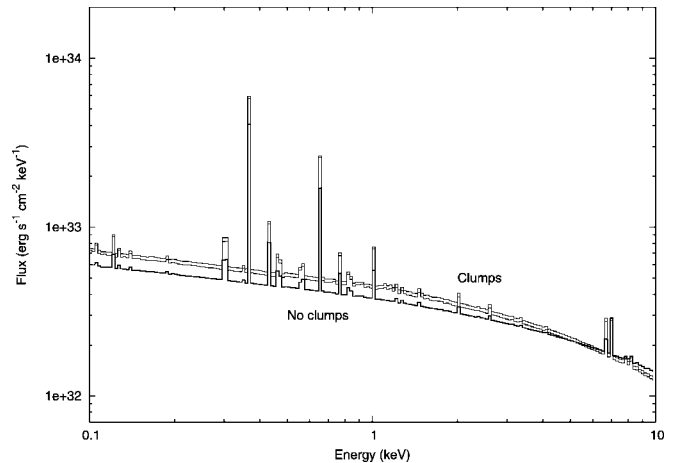


FIG. 3.—Comparison of the X-ray emission from simulations with homogeneous (*thick line*) and clumpy (*thin lines*) winds. The latter is slightly softer and shows only weak variability ( $\leq 5\%$ ), despite the fact that the hydrodynamic grid is not large enough to capture all of the emission (note the lack of lines below 1 keV). The emission was calculated using the MEKAL code (Mewe et al. 1995 and references therein), for optically thin thermal plasma, ionization equilibrium, and identical ion and electron temperatures.

### 4.1. Particle Acceleration and Synchrotron Emission

The radio synchrotron emission from wide CWBs has recently been modeled assuming that relativistic electrons are created by diffusive shock acceleration (DSA) at the shocks confining the WCR (Dougherty et al. 2003; Pittard et al. 2006; Pittard & Dougherty 2006). In the case of WR 140, Pittard & Dougherty (2006) find that the nonthermal (NT) electron energy distribution is harder than the canonical DSA value; i.e.,  $p < 2$ . While there are many possible explanations, the results presented above hint at several mechanisms. First, NT particles may be accelerated via the second-order Fermi process resulting from clump-induced MHD turbulence within the WCR (e.g., Scott & Chevalier 1975). Second, particles accelerated at the confining shocks may be reaccelerated at multiple (weak) shocks within the WCR (Schneider 1993). A third possibility is magnetic reconnection, which probably occurs throughout the volume of the turbulent WCR and not just at a hypothetical contact discontinuity. Reconnection may also provide additional energy for generating and maintaining the magnetic fluctuations that drive stochastic acceleration. If any of these mechanisms is dominant, models that impose particle acceleration only at the confining shocks will need to be revised accordingly. In addition, the magnetic field within the WCR is likely to be highly “tangled” due to the turbulent motions of the gas inside. This was a central assumption in the recent models mentioned above and means that the asymmetric radio light curve of WR 140 cannot be explained by the angular dependence of the synchrotron emission process.

### 4.2. Plasma Timescales

There are a variety of timescales within the WCR that may be modified if the stellar winds are clumpy (e.g., Walder & Folini 2002). In wide CWB systems, the shocks are collisionless, and the electron and ion temperatures may differ (an effect that appears to be sensitive to the shock speed; e.g., Hwang et al. 2002). Equilibration subsequently occurs through Coulomb collisions, proceeding faster where the density is higher, such as in material within the shocked clumps. The spectral hardness is sensitive to this process, but the overall flux is not dramati-

ically changed, and it is unlikely to have a significant impact on mass-loss rate determinations.

Ionization equilibrium may also take a significant time to occur. Direct evidence for nonequilibrium ionization is seen in WR 140 (Pollock et al. 2005), and models that assume ionization equilibrium fail to reproduce observed X-ray line profiles (Henley et al. 2005). Material originally within clumps will ionize quicker than interclump material, but to lower stages due to the reduced postshock temperatures. The relevant time-scale to obtain the highest ionization stages then becomes the speed at which further heating occurs in the downstream flow, through compressions, shocks, and mixing. The details are again sensitive to the clump properties, but the continuum emission, and thus estimates of  $\dot{M}$ , should not be strongly affected.

#### 4.3. Dust Formation

The highly turbulent interior of the WCR shown in Figure 1 enhances the mixing between the two winds. Such mixing may be necessary in order that carbon-rich WR material and hydrogen-rich O star material can form dust within the WCR (e.g., Walder & Folini 2002).

### 5. SUMMARY

The interaction of clumpy stellar winds in massive binary systems creates a highly turbulent wind-wind collision region in the adiabatic limit. The lifetime of clumps within the WCR depends on their density contrast and size. Clumps with a den-

sity contrast of 10 and radii a few times smaller than the half-width of the WCR on the line of centers between the stars are rapidly destroyed. Material originally within the clumps is then vigorously mixed into the surrounding flow.

The stochastic impact of clumps on the WCR and their subsequent destruction creates significant density and temperature fluctuations within the WCR, but the global X-ray emission can be remarkably similar to the smooth winds case. The X-ray emission is then an effective, clumping-independent, measure of the stellar mass-loss rates, especially if the wind momentum ratio is known. The small number of CWB systems suitable for such an analysis is countered by the potential accuracy that can be obtained. Each time this method has been used to determine mass-loss rates, values lower than those in the literature were inferred. Although only a small part of parameter space is explored here, any reasonable parameters for the clumps in the wide, adiabatic, systems considered here should lead to their rapid dissolution.

Turbulence and weak shocks within the WCR provide mechanisms for obtaining hard NT particle spectra. The timescale to obtain high-ionization stages may be controlled by the rapidity of clump destruction, and enhanced mixing of the winds will aid dust formation.

The author thanks the Royal Society for funding, Sam Falle for use of his hydro code, and Tom Hartquist, Sean Dougherty, Ian Stevens, and the referee for comments.

### REFERENCES

- Aleksandrova, O. V., & Bychkov, K. V. 2000, *Astron. Rep.*, 44, 781  
 Antokhin, I. I., Marchenko, S. V., & Moffat, A. F. J. 1995, in *IAU Symp.* 163, *Wolf-Rayet Stars*, ed. K. A. van der Hucht & P. M. Williams (Dordrecht: Kluwer), 520  
 Bouret, J.-C., Lanz, T., & Hillier, D. J. 2005, *A&A*, 438, 301  
 Dougherty, S. M., Beasley, A. J., Claussen, M. J., Zauderer, B. A., & Bolingbroke, N. J. 2005, *ApJ*, 623, 447  
 Dougherty, S. M., Pittard, J. M., Kasian, L., Coker, R. F., Williams, P. M., & Lloyd, H. M. 2003, *A&A*, 409, 217  
 Eversberg, T., Lepine, S., & Moffat, A. F. J. 1998, *ApJ*, 494, 799  
 Falle, S. A. E. G., & Komissarov, S. S. 1996, *MNRAS*, 278, 586  
 Fullerton, A. W., Massa, D. L., & Prinja, R. K. 2006, *ApJ*, 637, 1025  
 Henley, D. B., Stevens, I. R., & Pittard, J. M. 2005, *MNRAS*, 356, 1308  
 Hwang, U., Decourchelle, A., Holt, S. S., & Petre, R. 2002, *ApJ*, 581, 1101  
 Klein, R. I., McKee, C. F., & Colella, P. 1994, *ApJ*, 420, 213  
 Lamontagne, R., Moffat, A. F. J., Drissen, L., Robert, C., & Matthews, J. M. 1996, *AJ*, 112, 2227  
 Lepine, S., et al. 2000, *AJ*, 120, 3201  
 Marchenko, S. V., Moffat, A. F. J., St.-Louis, N., & Fullerton, A. W. 2006, *ApJ*, 639, L75  
 Mewe, R., Kaastra, J. S., & Liedahl, D. A. 1995, *Legacy*, 6, 16  
 Moffat, A. F. J. 1994, *Rev. Mod. Astron.*, 7, 51  
 Moffat, A. F. J., Drissen, L., Lamontagne, R., & Robert, C. 1988, *ApJ*, 334, 1038  
 Oskinova, L. M., Feldmeier, A., & Hamann, W.-R. 2006, *MNRAS*, 372, 313  
 Owocki, S. P., & Cohen, D. H. 2006, *ApJ*, 648, 565  
 Pittard, J. M. 2007, in *Diffuse Matter from Star Forming Regions to Active Galaxies*, ed. T. W. Hartquist et al. (Dordrecht: Springer), 245  
 Pittard, J. M., & Corcoran, M. F. 2002, *A&A*, 383, 636  
 Pittard, J. M., & Dougherty, S. M. 2006, *MNRAS*, 372, 801  
 Pittard, J. M., Dougherty, S. M., Coker, R. F., O'Connor, E., & Bolingbroke, N. J. 2006, *A&A*, 446, 1001  
 Pollock, A. M. T., Corcoran, M. F., Stevens, I. R., & Williams, P. M. 2005, *ApJ*, 629, 482  
 Puls, J., Markova, N., Scuderi, S., Stanghellini, C., Taranova, O. G., Burnley, A. W., & Howarth, I. D. 2006, *A&A*, 454, 625  
 Runacres, M. C., & Owocki, S. P. 2005, *A&A*, 429, 323  
 Schneider, P. 1993, *A&A*, 278, 315  
 Scott, J. S., & Chevalier, R. A. 1975, *ApJ*, 197, L5  
 Stevens, I. R., Corcoran, M. F., Willis, A. J., Skinner, S. L., Pollock, A. M. T., Nagase, F., & Koyama, K. 1996, *MNRAS*, 283, 589  
 St.-Louis, N., Moffat, A. F. J., Drissen, L., Bastien, P., & Robert, C. 1988, *ApJ*, 330, 286  
 Walder, R., & Folini, D. 2002, in *ASP Conf. Ser. 260, Interacting Winds from Massive Stars*, ed. A. F. J. Moffat & N. St.-Louis (San Francisco: ASP), 595